Effect of interfacial transport on the diffusivity of highly filled polymers

Colloid and Interface Science Communications 42 (2021) 100405

Contents lists available at ScienceDirect

Colloid and Interface Science Communications

journal homepage: www.elsevier.com/locate/colcom

Rapid Communication

Effect of interfacial transport on the diffusivity of highly filled polymers

M. van Soestbergen [a,*], A. Herrmann [b], S.J.F. Erich [b,c], O.C.G. Adan [b,c]

[a] NXP Semiconductors, Package Innovation, Gerstweg 2, 6534 AE Nijmegen, the Netherlands
[b] Department of Applied Physics, Eindhoven University of Technology, P.O. Box 513, 5600 MB, the Netherlands
[c] TNO, P.O. Box 49, 2600 AA Delft, the Netherlands

ARTICLE INFO

Keywords:
Interface transport
Diffusion
Polymer composites
Close packing of spheres
Tortuosity

ABSTRACT

The diffusivity of substances, such as moisture, through polymer composites is often described by an effective macroscopic quantity, even though microscopically the diffusivity might be far from uniform. In this work, we study the theoretical example of a permeable matrix containing equal-sized impermeable spheres. We assume that, due to interface effects, the diffusivity of the matrix in the vicinity of the spheres is higher than its bulk matrix diffusivity. Using numerical simulations of the composite's diffusivity, we show that upon the formation of large clusters of the highly permeable interfaces, i.e. near percolation of the spheres, the diffusivity of the composite rises sharply. For even higher values of the volume fraction of the spheres, up to the close-packing limit, the diffusivity decreases due to the increased tortuosity. This effect is well described by an analytical solution for the composite's diffusivity.

The diffusivity of polymers filled with additives (i.e. polymer composites) plays an important role in many branches of science and engineering. Examples of applications where moisture and/or ion diffusion plays an important role are, amongst many others, pigmented coating layers [1], optical silicones filled with phosphor particles for LED lighting [2], or highly-filled epoxies used to encapsulate microelectronic devices [3]. In general, the addition of fillers will affect the overall diffusivity of the polymer, as the fillers may have transport properties different compared to the matrix. Polymers blended with wood fillers, for example, show an increasing overall diffusivity for an increasing volume fraction of the fillers [4], due to the higher hydrophilicity of the fillers. In a similar fashion, fillers are added to polymers to enhance their thermal [5] and/or electrical conductivity [6], which increases significantly by aggregation of the fillers into clusters. In this letter, however, we will study the effect of impermeable fillers on the overall diffusivity of polymer composites. This e.g. resembles the case of microelectronic encapsulants, which are epoxies that are highly filled (up to ~80% volume fraction) with silica filler particles. Jansen et al. [7] argue that their moisture diffusivity is of the same order of magnitude as the diffusivity of unfilled epoxies, which is remarkable as for these high filler fractions one would expect a significantly lower diffusivity. Namely, Ahn et al. [8] report experimental data on similar encapsulants that indicate that the diffusivity decreases by a factor of ~2 for an increase in filler volume fraction from ~60% to ~80% alone. Their data also suggest that the presence of an adhesion promotor for bonding of the filler in the polymer matrix influences the diffusivity significantly. This suggests that interfacial transport along the filler interface has a significant impact on the overall diffusivity. Wapner et al. [9] used in-situ infrared spectroscopic and a scanning Kelvin probe, and found that water diffusion along an epoxy-iron interface was two orders of magnitude higher that bulk diffusion. Motta et al. [10] found a 30 times higher interfacial ion diffusivity for silica fillers embedded in epoxy mold compound using a charge induced transport experiment. Rocha et al. [11] studied a fiber-reinforced epoxy and found that a fit between macroscopic numerical simulations and experimentally data for the overall diffusivity was only possible when introducing a 1.5–3.5 times higher interfacial diffusivity compared to the bulk for a 1–4 μm thick interface region around the glass fibers. Molecular dynamics simulation by Dutta and Bhatia revealed the presence a ~1 nm thick interfacial layer where the diffusivity was either enhanced, up to 2 orders of magnitude [12], or reduced [13] depending on the local chemistry.

In this letter we report on both a numerical study and an analytical solution for a system containing a permeable matrix and impermeable spherical filler particles with an adjacent layer for mimicking the enhanced interface diffusivity. The aim is to show how an enhanced interfacial diffusivity affects the overall effective diffusivity of filled polymer composites.

For the numerical study we utilize representative volume elements

* Corresponding author.
E-mail address: Michiel.van.soestbergen@nxp.com (M. van Soestbergen).

https://doi.org/10.1016/j.colcom.2021.100405
Received 14 February 2021; Received in revised form 23 March 2021; Accepted 26 March 2021
Available online 19 April 2021

(RVEs), which were built using the commercial software Digimat. In each RVE 30 equal-sized spherical fillers were generated, where the size of the RVE was adjusted to obtain the designated volume fraction. RVEs were generated with volume fractions, ϕ, ranging from 0.05 up to the close-packing limit, i.e. $\phi_{cp} = \pi/3\sqrt{2} \approx 0.74$. For low volume fractions, the fillers were placed randomly (Fig. 1A), for volume factions approaching the random packing limit (i.e. $\phi \approx 0.6$) [14] the software automatically transitioned the RVEs into a face-centered cubic structure (Fig. 1B). The filler radius, R, varied from 2.5 up to 10 with 2.5 intervals (note that a dimensionless approach is used throughout this letter). A non-conformal voxel mesh was applied with a 0.5 size. To compute the effective diffusivity of the RVEs, the commercial finite element software MSC Marc was used to solve the equation for steady-state (Fickian) diffusion, i.e. $\nabla \cdot D_k \nabla C = 0$, where D_k is the diffusivity in material k and C is the solute concentration. Within the finite element simulation, the elements of the fillers are discarded, because they are assumed impermeable. The first layer of elements within the matrix originally adjacent to the fillers, i.e. the outmost layer of finite elements in the remaining numerical mesh, is regarded as the filler-matrix interface. Considering the above-mentioned element size, this thus results in an interface layer thickness of 0.5. Next, a concentration of 1 is set to one face of the RVE ($C_1 = 1$), whereas the flux is computed at the opposite face, where the concentration is zero ($C_0 = 0$). On all other faces, a symmetry boundary condition is applied.

The effective diffusivity of the RVE, D_e, is a macroscopic quantity defined as, $D_e = J_n/(\nabla C \, \boldsymbol{n})$, where J_n is the total flux per total face area through the RVE face at zero concentration, $\boldsymbol{n}$ is its outward normal, and ∇C is the concentration gradient across the RVE, which equals $(C_1 - C_0)/L_{RVE} = 1/L_{RVE}$, with L_{RVE} the RVE length. The computed results for the effective diffusivity of the RVE with a filler radius of 5 are given in Fig. 2. Here the diffusivity of the matrix is set to 1 and the diffusivity of the interface, D_i, is varied from 1 to 100. For $D_i = 1$ (no enhanced interface diffusivity) the effective diffusivity decreases monotonically as a function of the filler volume fraction due to the increasing tortuosity, τ, of the system, and a decreasing amount of matrix material. For higher values of D_i the effective diffusivity of the RVE first increases due to the beneficial effect of the enhanced interface diffusivity, whereas close to the random packing limit D_e decreases again. The inset of Fig. 2 shows the effective diffusivity corrected for the tortuosity of the system as a function of the interface diffusivity (the tortuosity can be derived from the results at $D_i = 1$ as explained below). For low values of the filler volume fraction D_e increases non-linearly with increasing D_i. For low filler volume fraction the effective diffusivity is given by the dilute mixture theory of impermeable fillers in a permeable matrix with an interface layer in between, which is intrinsically non-linear [1]. For high values of the filler volume fraction a high diffusivity path throughout the RVE is formed due to overlapping interface layers. Once sufficient overlap is achieved, $D_e \cdot \tau$ increases near linear with increasing values for D_i.

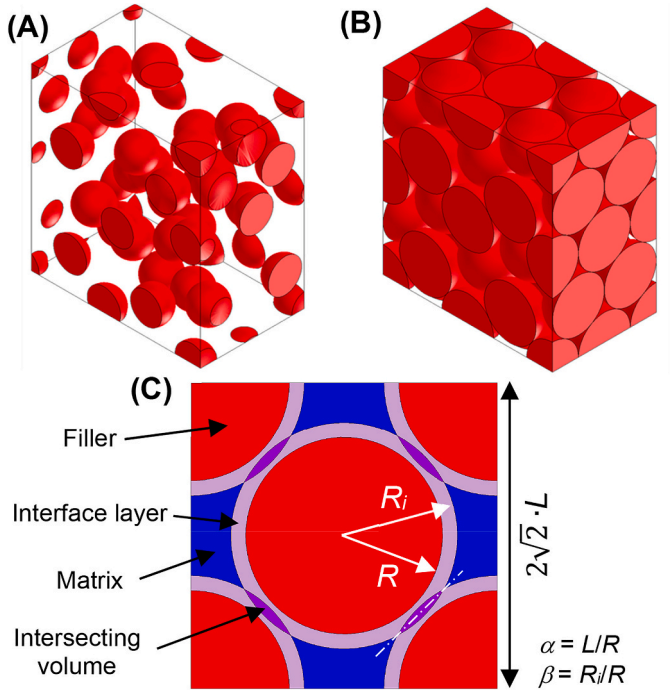

Fig. 1. (A) RVE for $R = 5$ and $\phi = 0.2$ showing the random filler distribution; (B) RVE for R = 5 and $\phi = 0.74$ showing close packing; (C) schematic showing a face of the face-centered cubic structure.

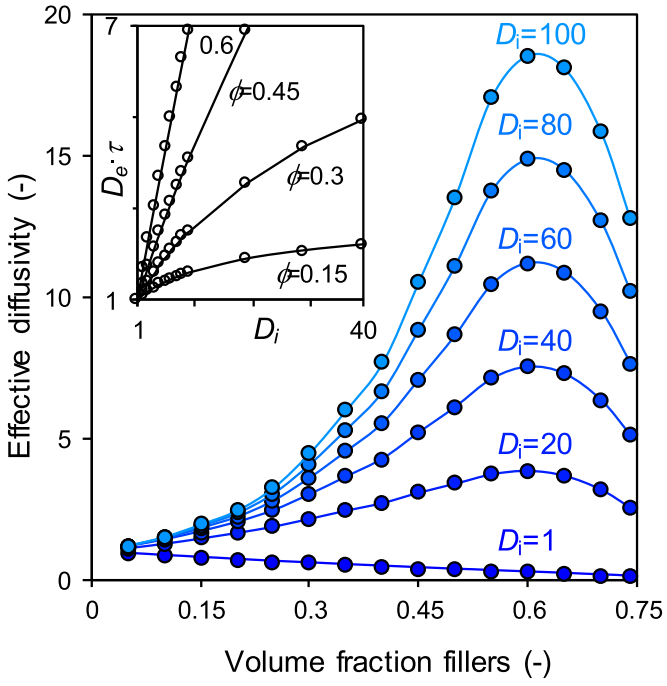

Fig. 2. Results from the numerical study showing the effective diffusivity as a function of the filler volume fraction for different values of the interface diffusivity, matrix diffusivity equal to 1, and $R = 5$. The inset shows the effective diffusivity normalized by the tortuosity as a function of the interface diffusivity. The lines are a guide to the eye.

To derive an analytical equation for the effective diffusivity, we first need to find a relation for the tortuosity as a function of the volume fraction of fillers. To determine the tortuosity as a function of the filler volume fraction from the results obtained for the RVEs we omit the enhanced interface diffusivity, so that the effective diffusivity can be written as $D_e = D_m(1 - \phi)/\tau$ (see e.g. ref. 15), and with $D_m = 1$ the tortuosity can be computed as $\tau = (1 - \phi)/D_e$. The corresponding results are given in Fig. 3A. There is no consensus in the literature on a unified model for the tortuosity of porous materials [16]. In this letter we follow the work by Ahmadi et al. [17] on the tortuosity of packed mono-sized spheres. They found that for cubic and tetrahedral packings the tortuosity is given by,

$$\tau = \sqrt{\frac{2(1-\phi)}{3[1 - B\phi^{2/3}]} + \frac{1}{3}} \tag{1}$$

where B depends on the structure of the packing (1.209 for cubic, and 1.108 for tetrahedral), and can be used as an adjustable parameter for other packing types. Eq. (1) correlates well with our numerical data derived from the RVEs for $B = 1.16$. Originally, Eq. (1) was originally developed for filler volume fractions ranging from 0 to 0.6 [17]. The fit in this work shows that Eq. (1) approximates the rapid increase in

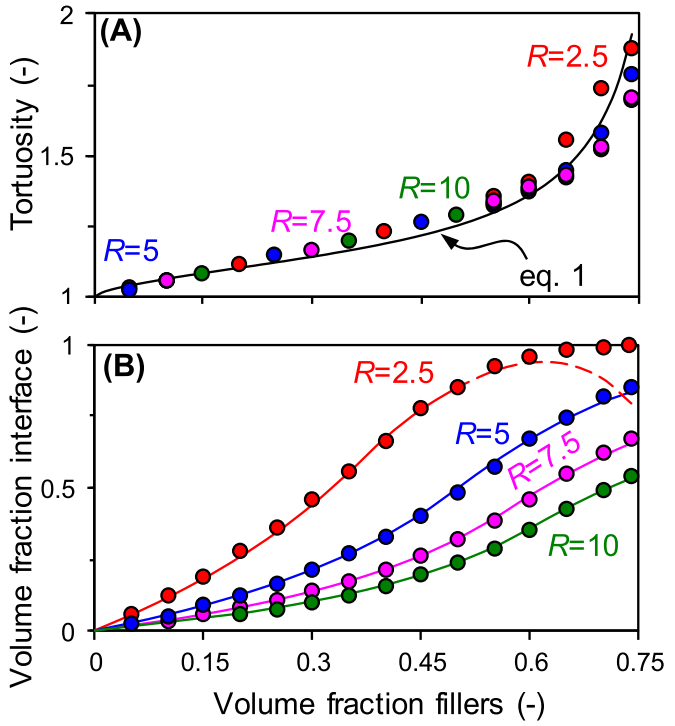

Fig. 3. (A) Tortuosity as a function of the volume fraction of the fillers for different filler radii. The solid line is a fit to the data according to Eq. (1) with B = 1.16. (B) Volume fraction of the interface layer as found from the finite element models of the RVEs (markers), and the corresponding results for the analytical solution of Eq. (5) (solid lines). The dashed line indicates the physical irrelevant solution for Eq. (5).

tortuosity after $\phi \approx 0.6$ well for the monodisperse systems used in this work. For polydisperse systems, such as used in ref. 8, the filler size distribution must be considered as e.g. discussed in 16.

Next, we develop an analytical relation for the effective diffusivity as a function of the filler volume fraction. Here several approaches are possible. Donkers et al. [1] derived an analytical equation for the diffusivity of a permeable spherical particle in an infinite matrix with an interface layer in between. This approach can only be used for dilute mixtures. Jia et al. [18] determined the properties of an equivalent particle for a multi-layered hollow sphere and they subsequently substituted these properties in common equations for the effective thermal conductivity of binary mixtures. In this letter, however, we follow the generalized effective medium theory developed by McLachlan [19], which can be viewed as a matched asymptotic expression of the equations for the electrical conductivity from the percolation theory for two individual conductive systems [20]. Replacing the electrical conductivity in McLachlan's theory by the corresponding diffusivities gives the implicit relation [8],

$$\phi_i \frac{D_i^{1/n} - D_b^{1/n}}{D_i^{1/n} + xD_b^{1/n}} + (1-\phi_i)\frac{D_m^{1/m} - D_b^{1/m}}{D_m^{1/m} + xD_b^{1/m}} = 0 \tag{2}$$

where ϕ_i is the volume fraction of the interface layer within the matrix, D_b is the diffusivity of the binary mixture (matrix + interface), n and m are fitting constants, and $x = 1/\phi_{cr} - 1$, with ϕ_{cr} called the 'critical' volume fraction in ref. 19, which is used as an adjustable parameter in this work. When we assume $n = m$, and $D_m = 1$, we can write Eq. (2) into an explicit relation for D_b, and find the effective diffusivity of the RVEs by dividing D_b by the tortuosity of the total system, which yields,

$$D_e = \frac{1}{\tau}\sqrt[n]{\frac{P}{2x} + \sqrt{\left(\frac{P}{2x}\right)^2 + \frac{D_i^{1/n}}{x}}} \tag{3}$$

where $P = \phi_i(xD_i^{1/n} - 1) + (1 - \phi_i)(x - D_i^{1/n})$.

Eq. (3) is still a function of the interface volume fraction. To write Eq. (3) as a function of the filler volume fraction we need to find ϕ_i as a function of ϕ. In order to do this, we consider the case of the face-centered cubic structure, for which one of the faces of its unit cell is depicted in Fig. 1C. The unit cell has 6 halve spheres at the center of its faces and 8 times an 1/8 sphere at its corners, which equals 4 spheres in total. The volume of the interfacial shell around these spheres thus equals $V_{sh} = 4\frac{4}{3}\pi\left(R_i^3 - R^3\right) = \frac{16}{3}\pi R^3\left(\beta^3 - 1\right)$, where $\beta = R_i/R$ with R_i the outer radius of the spherical shell that defines the interfacial layer. At high volume faction the interfacial layers will partly overlap as depicted in Fig. 1C. Therefore, we will derive a function for the intersecting volume. First, we denote the length of the edges of the unit cell as $2\sqrt{2}\cdot L$ and define $L = \alpha R$. The volume of a spherical filler equals $V_{sp} = \frac{4}{3}\pi R^3$. Consequently, the volume fraction of the fillers in the unit cell is given by $\phi = 4V_{sp}/V_{cell} = \pi/\left(3\sqrt{2}\alpha^3\right)$ from which follows that $\alpha = \sqrt[3]{\phi_{cp}/\phi}$. Next, note that the intersecting volume equals two times the spherical cap as cut off by the dashed line in Fig. 1C. The volume of this cap is given by $V_{cap} = \frac{1}{3}\pi h^2(3R_i - h)$, where h denotes the height of the cap, which in our case equals $h = R_i - L = R(\beta - \alpha)$. The 8 corner spheres have each 3 unique points where overlap occurs, but only at half-symmetry, whereas the 6 halve spheres touch each other at 4 points, which brings the total intersecting volumes at $N = 24$. As a result, the total intersecting volume equals,

$$V_i = \frac{16}{3}\pi R^3\left(\beta^3 - 1\right) - \frac{2N}{3}\pi R^3(\beta - \alpha)^2(2\beta + \alpha) \tag{4}$$

Finally, the volume fraction of the interface layer within the matrix is defined as, $\phi_i = V_i/[V_{cell}(1 - \phi)]$, which after substitution of Eq. (4) results in

$$\phi_i = \frac{\phi}{1-\phi}\left[\left(\beta^3 - 1\right) - \frac{N}{8}(\beta - \alpha)^2(2\beta + \alpha)\right] \tag{5}$$

Results for ϕ_i for the RVEs and according to Eq. (5) are plotted in Fig. 3B. Both the fillers and the interface layers are not perfectly spherical in the RVEs, because of the 0.5-sized voxel mesh, which is more pronounced for the smaller fillers. Therefore, R and R_i, thus effectively β, were used as fitting parameters, which resulted in β equal to 1.27, 1.14, 1.10, and 1.07 for R equal to 2.5, 5, 7.5 and 10, respectively. Overlap of the interface layers is assumed to start at the volume fraction where the interface layers start to touch. Considering Fig. 1C, the onset of overlap occurs at a diagonal length of $4\beta R$ which equals $4L = 4\alpha R$. Consequently, the onset occurs at $\alpha = \beta$, which is equal to $\phi = \phi_{cp}/\beta^3$, and ϕ is 0.37, 0.50, 0.56, and 0.60 for R equal to 2.5, 5, 7.5 and 10, respectively. Below these values no touching is assumed, i.e. $N = 0$, and above these values $N = 24$, as mentioned above. For high values of β, triple points in the overlap of the interfaces can occur [21], which is not considered in Eq. (5) for the sake of simplicity. For a body-centered cubic structure this limit will be reached at $\phi = 9\pi/32\beta^3$ (see ref. 21), which yields 0.51 for our case of $R = 2.5$. Beyond this value Eq. (5) overcompensates for the interface overlap, and the volume fraction of the interface layer is predicted to decrease with increase volume fraction of the fillers as indicated by the dashed line in Fig. 3B. This part of Eq. (5) is thus considered physically irrelevant. Therefore, we consider Eq. (5) to be accurate for fillers with a thin interfacial layer, which will be the case for most practical applications.

The results for the tortuosity (Eq. (1)) and volume fraction of the interface layer (Eq. (5)) are substituted in Eq. (3) to compute the effective diffusivity of the four RVEs, as shown in Fig. 4. Here n and ϕ_{cr} are used as fitting parameters. For n the values of 1.23, 1.04, 0.98, and 0.95 are found, and for ϕ_{cr} the values of 0.209, 0.187, 0.147, and 0.119 are found, for R equal to 2.5, 5, 7.5 and 10, respectively. These numbers are in the range of those reported in ref. 19. The results of the analytical equations fit reasonably well with the numerical results of the RVEs.

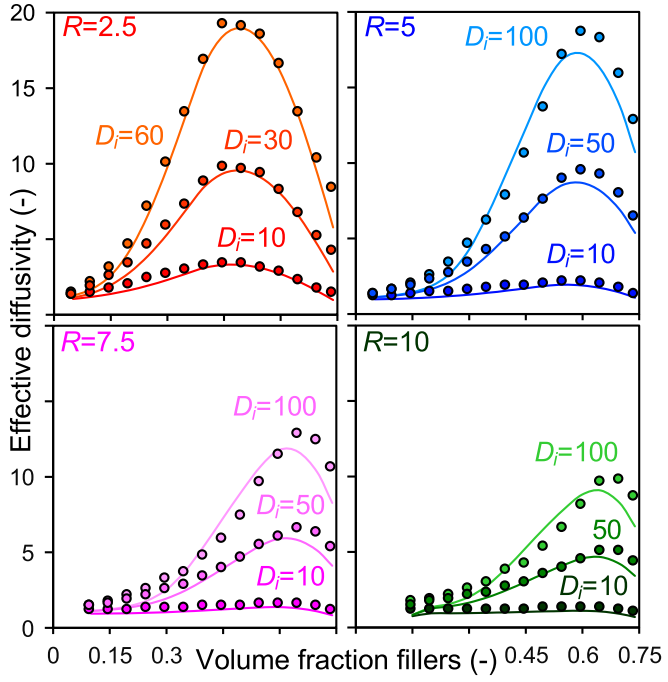

Fig. 4. The effective diffusivity as a function of the volume fraction of fillers for four different radii of the spherical filler particles; the markers show the numerical results of the RVEs, and the solid lines represent the fit according to Eqs. (1), (3) and (5) with fitting parameters as given in the text.

Both the numerical and analytical results show a rapid increase in diffusivity upon reaching the percolation limit, theoretically at $\phi \approx 0.29$ for a "Swiss cheese" structured model with mono-sized spheres [22]. Both results also show a peak in diffusivity around the volume fraction where overlap of interfacial layers starts to occur. This latter point depends on the radius of the filler particle. The reduction in effective diffusivity at high ϕ is not solely driven by the rapidly increase in tortuosity after $\phi \approx 0.6$ (see Fig. 3A), but is also driven by the reduced growth in the volume fraction of the interface fraction at high ϕ. This second effect becomes dominant for larger values of β.

To study the effect of the interfacial layer thickness on the effective diffusivity, n and ϕ_{cr} are fitted to linear functions (Fig. 5A). The fits are used to determine $D_e{\cdot}\tau$ as a function of β-1 for various values of the interfacial diffusivity (Fig. 5B). These results show that for micrometer-sized fillers with and interfacial layer thickness in the order of nanometers (β-1 $\approx 10^{-3}$) a two order of magnitude enhanced interface diffusivity is needed to significantly increase $D_e{\cdot}\tau$. Likewise, for thicker interface layers a much lower enhanced diffusivity leads to the same increase in $D_e{\cdot}\tau$. This might explain the discrepancy between the interface layer thickness found by fitting experimental data for the effective diffusivity to macroscopic models [11], and the theoretical thickness found by molecular dynamics simulations [12,13].

To conclude: enhanced interfacial diffusivity can play a dominant role in the effective macroscopic diffusivity of highly filled composite. The resulting macroscopic diffusivity does not only depend on the tortuosity of the composite and the interfacial diffusivity, but also on the volume fraction of the interface layer and the formation aggregates.

Author statement

All authors have seen and approved the final version of the manuscript being submitted. We warrant that the article is the authors' original work, hasn't received prior publication and isn't under consideration for publication elsewhere.

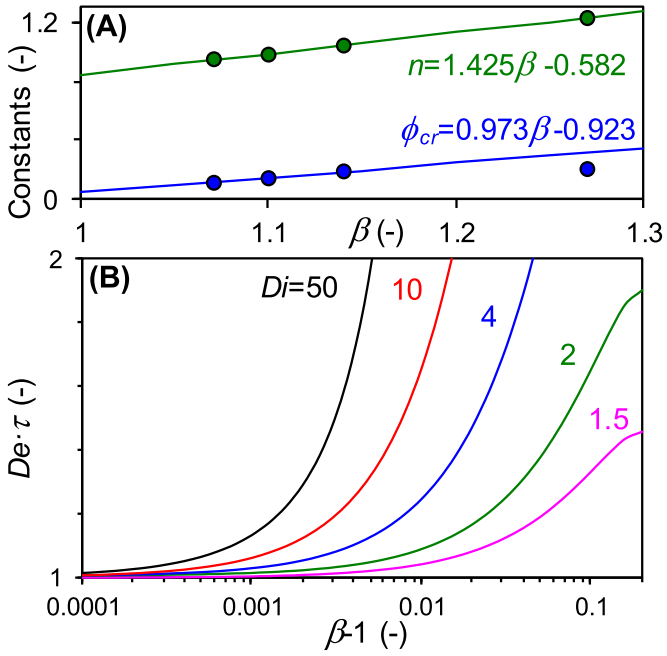

Fig. 5. (A) Fitting parameters used in Eq. (3) as a function of the interface layer thickness ratio. (B) Effective diffusivity normalized by the tortuosity as a function of the normalized interface layer thickness for various values of the interface diffusivity.

Declaration of Competing Interest

The authors declare that they have no competing financial interests or personal relationships that could have appeared to influence the work reported in this paper.

References

[1] P.A.J. Donkers, H.P. Huinink, S.J.F. Erich, N.J.W. Reuvers, O.C.G. Adan, Progr. Organ. Coat. 76 (2013) 60–69.
[2] A. Herrmann, S.J.F. Erich, L.G.J. V.D. Ven, H.P. Huinink, W.D.M. van Drielvan Soestbergen, A. Mavinkurve, F. De Buyl, J.M.C. Mol, O.C.G. Adan, Optic. Mater. X 6 (2020) 100047.
[3] M. van Soestbergen, A. Mavinkurve, R.T.H. Rongen, K.M.B. Jansen, L.J. Ernst, G. Q. Zhang, Electrochim. Acta 55 (2010) 5459–5469.
[4] M.A. Almaadeed, Z. Nógellová, M. Micušík, I. Novák, I. Krupa, Mater. Des. 53 (2014) 29–37.
[5] W. Evans, R. Prasher, J. Fish, P. Meakin, P. Phelan, P. Keblinski, Int. J. Heat Mass Transf. 51 (2008) 1431–1438.
[6] S.-H. Park, J. Hwang, G.-S. Park, J.-H. Ha, M. Zhang, D. Kim, D.-J. Yun, S. Lee, S. H. Lee, Nat. Commun. 10 (2019) 2537.
[7] K.M.B. Jansen, M.F. Zhang, L.J. Ernst, D.-K. Vu, L. Weiss, Microelectron. Reliab. 107 (2020) 113596.
[8] W. Ahn, D. Cornigli, D. Varghese, L. Nguyen, S. Krishnan, S. Reggiani, M.A. Alam, IEEE Trans. Compon. Packag. Manufact. Technol. 10 (2020) 1534–1541.
[9] K. Wapner, M. Stratmann, G. Grundmeier, Electrochim. Acta 51 (2006) 3303–3315.
[10] V. Motta, M. Schäfer, F. Noll, N. Hampp, K.-M. Weitzel, ECS J. Solid State Sci. Technol. 9 (2020), 053001.
[11] I.B.C.M. Rocha, S. Raijmaekers, F.P. van der Meer, R.P.L. Nijssen, H.R. Fischer, L. J. Sluys, Compos. Sci. Technol. 151 (2017) 16–24.
[12] R.C. Dutta, S.K. Bhatia, J. Phys. Chem. C 124 (2020) 594–604.
[13] R.C. Dutta, S.K. Bhatia, ACS Appl. Mater. Interfaces 10 (2018) 5992–6005.
[14] M.M. Levine, J. Chernick, Nature 208 (1965) 68–69.
[15] J.M. Zalc, S.C. Reyes, E. Iglesia, Chem. Eng. Sci. 59 (2004) 2947–2960.
[16] B. Ghanbarian, A.G. Hunt, R.P. Ewing, M. Sahimi, Soil Sci. Soc. Am. J. 77 (2013) 1461–1477.
[17] M.M. Ahmadi, S. Mohammadi, A.N. Hayati, Phys. Rev. E 83 (2011), 026312.
[18] Z. Jia, Z. Wang, D. Hwang, L. Wang, ACS Appl. Energy Mater. 1 (2018) 1146–1157.
[19] D.S. McLachlan, Solid State Commun. 60 (1986) 821–825.
[20] J. Kováčik, Scr. Mater. 39 (1998) 153–157.
[21] S. Raetzke, J. Kindersberger, IEEE Trans. Dielectr. Electric. Insulat. 17 (2010) 607–614.
[22] C.D. Lorenz, R.M. Ziff, J. Chem. Phys. 144 (2001) 3659–3661.